Proceeding of the IEEE
International Conference on Robotics and Biomimetics
Dali, China, December 2019

Visual Road Boundary Detection based Local Path Planner*

Ning Li[1], Xijun Zhao, Bo Su[2]

China North Vehicle Research Institute

Beijing, 100072, China

[1]lining199003@163.com

[2]bosu@noveri.com.cn, corresponding author

[3]Zhiqing Wang

College of information science and electric engineering
Zhejiang University
Hangzhou, 310058, China

[3]wangzhiqing@zju.edu.cn

***Abstract* - We propose a real-time visual road detection based local path planner for autonomous navigation in unstructured environments. The system consists of two parts: road detection and local path planning. Road boundary model based on convolution neural network is trained for local road detection in image frame. After perspective transformation, the result is transformed to the vehicle's frame for path planning. The road midline generated from the road boundaries is used to represent the reference local path. Priori information with the global navigation topology map is combined to solve multi-roads selection. Finally, data fusion with historical detection results and predictive control of vehicle model is used for path optimization. In addition, obstacle avoidance combined with LIDAR perception is also taken into account to complete an autonomous navigation task in complex scenarios.**

A large number of experiments with various road conditions shows that the proposed method has a good adaptability and versatility for unstructured scenarios. The algorithm can effectively reduce the dependence on absolute positioning and LIDAR perception. So it is of great importance for autonomous navigation in scenarios without satellite or in unknown scenarios.

Index Terms* - *Autonomous Navigation, Road Detection, Unstructured Environments, Local Path Planning.

I. INTRODUCTION

Autonomous navigation technology is the focus of research for robotic applications [1-6] in recent years. In known scenarios, a hierarchical path planner including global routing planner and local motion planner is widely used for autonomous navigation from the starting point to the finishing point. In this manner, the global routing planner is responsible for generating tracking path based on the priori global map, meanwhile the local motion planner is just used for trajectory tracking and local obstacle avoidance. This method is widely applied in urban environments. Path tracking mainly depends on the high-precision map matching based on LIDAR, cameras and the precise absolute positioning within 2cm accuracy error such as RTK.

For unstructured environments, it is usually difficult to build a priori high-precision map due to the irregular road conditions and lack of regularized reference objects. In addition, due to the occlusion of trees or other obstacles, there is a poor satellite positioning in such scenarios. Wheel slippage is another factor that affects positioning accuracy. It causes harmful effects for dead reckoning of Inertial Measurement Unit (IMU). So the positioning accuracy of integrated navigation is not high. In unstructured environment with poor satellite signals or unknown scenarios without priori high-precision map information, it is difficult to achieve effective routing planning. Based on the above fact, path planning that rely solely on map matching and precise positioning are ineffective. Besides it is difficult to guarantee autonomous driving in the middle of the road. For unknown scenarios with a given sparse priori topological map, the hierarchical path planner mentioned above can hardly be applied.

In unstructured scenario, local road perception based local path planning is of great importance for autonomous navigation. Paper [7] presents a road boundary detection method based on LIDAR perception, in which road plane hypothesis and boundary gradient information statistics is important pre-processing. The method can be used for local path planning in urban traffic system with structure road environment. But for unstructured environment with rough terrain, for example, country roads with low grass on both sides and in the middle as shown in Fig. 1, it is difficult to effectively detect road edge features or road surface feature just by LIDAR. Only a few grasses with large height can be detected as road boundaries, so road extraction by LIDAR is too hard.

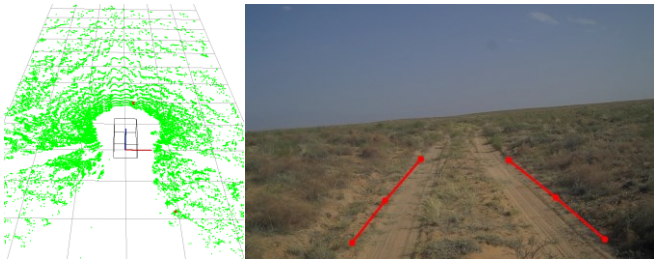

(a) (b)

Fig.1: (a) Point cloud. (b) Visual road boundary detection.

However, using visual texture features, the road boundary information can be well recognized in Fig. 1(b). In paper [8], vision based road detection is used for autonomous navigation in unstructured environment. Image segmentation based on OTSU is used for road extraction, and the road midline is

*Research supported by the National Natural Science Foundation of China (Grant No. 91748211).

978-1-7281-6321-5/19//$31.00 ©2019 IEEE

obtained by statistics of the extracted road plane. The traditional image processing method is more severely affected by illumination and terrain, and it has a poor adaptability to complex scenarios such as grass in the middle of the road as shown in Fig. 1(b). Besides the problem of multi-roads selection is not included in their work. This problem must be considered for a complete autonomous navigation task.

II. Our Work

For autonomous navigation in unstructured scenarios, our research is also mainly based on visual detection like [8]. But the detailed road detection method and the post-processing of path generation are different from that in paper [8]. First, we adopt a deep learning framework of Convolutional Neural Network to extract road boundaries. Training samples includes a plenty of typical unstructured scenarios including country road, forest road, desert road and paved road. Shaded roads are also considered. Road shape includes one-way road, curve road and fork road. The proposed method is more versatile for all kinds of unstructured scenarios with clear or blurred road boundaries. Local road guidance path can be generated by the visual road boundaries denoted as polylines shown in Fig. 1(b).

Compared with structured roads in urban environments, road boundaries in unstructured environment is difficult to be extracted accurately, so a robust local path planner is essential, which is also the focus of this paper. In the proposed method, local tracking trajectories generation is associated with historical detection result not just the current detection result, it is useful to improve the stability of the path tracking. And predictive control based on vehicle model is also taken as a means of trajectories optimization to ensure smooth trajectories tracking, which is critical for the real-time autonomous navigation system. Meanwhile for multi-roads detection result, combined with the priori global navigation topological map (GNTM) and the vehicle's navigation information, the correct road to go can be selected. This is important for performing a complete autonomous navigation task from the starting point to the finish point.

The proposed visual road detection based local path planner has many advantages. It can effectively reduce dependence on precise global absolute positioning. Meanwhile it can guarantee the stability of vehicle's lateral control as the generated tracking path is along with the actual trend of the road all the time.

The remainder of this paper is organized as follows: Sec. III is the overview of the system. Sec. IV is the description of CNN based road boundary detection. Sec. V explains the implementation of local path planning. Sec. VI is the experiment and Sec. VII is the conclusion.

III. System Overview

Fig. 2 shows the diagram of visual road detection based local path planning system. The system consists of two parts. The first part is the road detection in a single image frame. Convolutional Neural Network based model is trained to predict the road boundaries in the image frame. After perspective transformation, the detection result is transformed into the vehicle's frame. The second part is in the vehicle's local frame. In this frame, road detection result is expressed as a linear equation for simplicity. For potential multi-roads selection issues, the correct road to go can be selected with the help of the GNTM combined with the vehicle's navigation information. To increase the stability of the self-driving control, path optimization by fusing historical frames and using predictive control of vehicle model is an important step in the proposed logical design. In addition, obstacle avoidance combined with LIDAR perception is also included in our research. It is essential to complete an autonomous navigation task in complex environment. The average processing rate of the algorithm is around 9Hz.

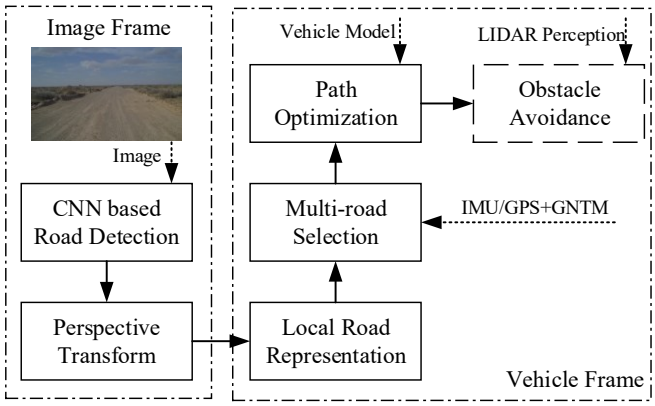

Fig. 2 Block diagram of visual road detection based local path planner.

IV. Visual Road Detection

Road boundary detection model is developed based on Convolutional Neural Network (CNN) architecture to adapt to complex scenarios in the proposed method. Training data including various road environments can ensure sufficient generalization for different environments.

A. CNN based Visual Road Boundary Detection Model

Each road boundary is represented by three discrete points in the training phase. The polyline connected with each group of three discrete points as shown in Fig. 1(b) is used to abstractly describe road boundaries. Compared with curve line representation with continuous points, the proposed boundary representation is simple during manual data annotation for model training. Besides, for unstructured road with irregular boundaries, this representation method is more robust.

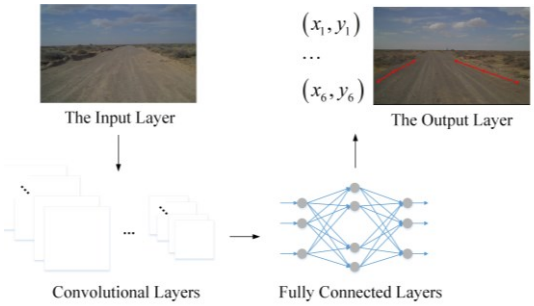

Fig. 3 Schematic diagram of CNN based road detection.

Refer to the method proposed in Paper [9], we use YOLO [10-12] based CNN detection model as the training model to detect the object. The input layer is a unified size image, and the output layer includes coordinates of 6 points represented as (xi, yi) located separately on each boundary (The first three represent the left boundary and the last three represent the right boundary). The convolutional layers are used to extract features from the input layer and fully connected layers are used to perform feature calculation for the final prediction. The schematic diagram is shown in Fig. 3.

B. Perspective Transformation solving

The visual road detection result is in the image frame while the local path planning is performed in the vehicle's frame. Thus it is necessary to calibrate the transformation relation between the above two frames. After that, the visual road boundary detection result can be mapped to the vehicle's frame for autonomous navigation. The transformation from the image frame to the vehicle's frame is called perspective transformation [13] as shown in (1):

$$[x', y', w'] = [u, v, w] \cdot R = [u, v, w] \cdot \begin{bmatrix} a_{11} & a_{12} & a_{13} \\ a_{21} & a_{22} & a_{23} \\ a_{31} & a_{32} & a_{33} \end{bmatrix} \quad (1)$$

Where (u, v) corresponds to the pixel coordinate in the image frame and w=1. (x, y) corresponds to the 2D Cartesian coordinate in the vehicle's frame and meets the constraint: $x = x'/w', y = y'/w'$. The matrix R is called the perspective transformation matrix.

Expanding (1), the relationship between the image frame and the vehicle's frame can be obtained as shown in (2):

$$\begin{cases} x = \dfrac{x'}{w'} = \dfrac{a_{11}u + a_{21}v + a_{31}}{a_{13}u + a_{23}v + a_{33}} \\ y = \dfrac{y'}{w'} = \dfrac{a_{12}u + a_{22}v + a_{32}}{a_{13}u + a_{23}v + a_{33}} \end{cases} \quad (2)$$

The perspective transform matrix includes 8 unknowns (a_{33}=1 is known). According to (2), the transformation matrix can be solved by using at least 4 groups of corresponding data.

In the experiment, we use conical buckets as the reference object between the image frame and the vehicle's frame. The front edge point of the conical bucket shown in Fig. 4(a) is chosen as the calibration reference point. The corresponding position in the vehicle's frame can be obtained by measurement. After parking the vehicle platform, some conical buckets are placed at locations with known distances both in the horizontal and vertical direction in the vehicle's frame. The reference point in the image is associated with the actual position in the vehicle's frame.

In order to reduce the calibration error, 8 or more conical buckets are placed in the same scenarios simultaneously. In our experiment, with the vehicle's width as the horizontal distance reference, 8 conical buckets are placed symmetrically at a distance of 10m, 20m, 30m in front of the vehicle. The distribution is shown in Fig. 4(a).

Taking the center of the rear axle of the vehicle body as the origin of the vehicle's frame, the relation between the conical buckets' positions in the vehicle's frame and the corresponding pixel positions in the image frame is shown in Table 1.

(a) (b)

Fig. 4: (a) Image. (b) Grid map in the vehicle's frame where one pixel represents the actual area of 0.2m2.

TABLE I Data for perspective transformation solving

Idx	Vehicle's frame (unit : m)	Image frame (unit : pixel)
1	(-2.5,10.00)	(253,459)
2	(-5.0,20.00)	(316,338)
3	(-5.0,30.00)	(477,311)
4	(0.0,30.00)	(746,320)
5	(5.0,30.00)	(1019,332)
6	(5.0,20.00)	(1168,369)
7	(2.5,10.00)	(1267,495)
8	(0.0,10.00)	(810,485)

According to the corresponding positional relationship of 8 conical buckets in two frames, the perspective transformation matrix can be solved by (2). Fig. 4(b) shows an aerial view of the image after perspective transformation.

V. LOCAL PATH PLANNER

A. Local Road Representation

By using perspective transformation, the detected road boundary points can be projected to the vehicle's frame as shown in Fig. 5(b). For the detected left and right road boundary points, the linear model can be used to obtain the boundary equation. In the actual processing, the straight linear equation is more robust than the parabolic linear equation. And for most straight roads, the line equation can effectively represent the road model. For the curve road, the slope of the linear equation can also be good for fitting the curvature of the road. The parabolic equation is prone to over-fitting for some irregular road sections in our data processing. So the linear equation model is chosen to describe the road boundary to improve robustness.

In the vehicle's frame, the road boundary is expressed by the linear equation shown in (3):

$$x = k \cdot y + b \tag{3}$$

As each road boundary is described by three points, the least square method is used to solve the overdetermined equations of each road boundary. And the singular value decomposition (SVD) is adopted for specific equation solving. For each road boundary, the input matrix of SVD is defined as the displacement deviation from given boundary points to their mean point as shown in (4):

$$A = P - M \tag{4}$$

Where $P = \begin{bmatrix} x_1 & y_1 \\ x_2 & y_2 \\ x_3 & y_3 \end{bmatrix}$, $M = \begin{bmatrix} \frac{x_1+x_2+x_3}{3} & \frac{y_1+y_2+y_3}{3} \\ \frac{x_1+x_2+x_3}{3} & \frac{y_1+y_2+y_3}{3} \\ \frac{x_1+x_2+x_3}{3} & \frac{y_1+y_2+y_3}{3} \end{bmatrix}$.

(a) (b)

Fig. 5: (a) Road boundary detection result in the image. (b) Road boundary result projected to the vehicle's frame.

By calculating (5), the parameters of each road boundary equation can be obtained separately.

$$A = U_{3\times3} \cdot \Sigma_{3\times2} \cdot V_{2\times2} \tag{5}$$

Where $U_{3\times3}$ and $V_{2\times2}$ are the square matrix consisting of the standard orthogonal basis. $\Sigma_{3\times2}$ is a diagonal matrix. The singular vector in $V_{2\times2}$ corresponding to the minimum singular value is chosen as the linear equation parameters. Each road boundary is described as a straight line crossing boundary points in Fig. 5(b).

Due to the bumpy in rough-terrain environments, the pitch and roll angles of the vehicle change greatly during driving. As a result, the visual detected result may not keep stable, especially after perspective transformation, the deviation will be magnified. As shown in Fig. 5(b), the left and right road boundaries cross together at about 30m which is inconsistent with the actual road situation.

Taking the symmetry of perspective transformation error of the two boundaries into account, the error caused by the vehicle tilting can be eliminated by calculating the center line of the two boundaries as shown in (6).

$$\begin{cases} x = k_L \cdot y + b_L \\ x = k_R \cdot y + b_R \end{cases} \Rightarrow \begin{cases} x = k_M \cdot y + b_M \\ k_M = (k_L + k_R)/2, b_M = (b_L + b_R)/2 \end{cases} \tag{6}$$

At the same time, the abstract expression model of the local road is represented by the road's middle-line equation. As shown in Figure 5, the trend of the road middle-line is basically the same along with the road's extension direction.

According to the vehicle's heading, we can also get the road orientation in the global coordinate system by the heading conversion relationship as shown in (7). It is useful for the next multi-roads selection problem.

$$\theta_G = \theta_L + \theta_v - \frac{\pi}{2} \tag{7}$$

Where θ_L is the road heading in the vehicle's frame, θ_v is the current driving heading, θ_G is the road orientation in the absolute global frame.

B. Multi-roads Selection

For the fork, multi-roads detection results are shown in Fig. 6(a). In addition, due to the irregularity of the unstructured roads, one-way roads may occasionally generate multi-roads detection results and thus it causes the multi-roads selection problem. In this case, the priori information of the global navigation topology map(GNTM) can play an important role in the selection of the correct road to go as shown in Fig. 6(c).

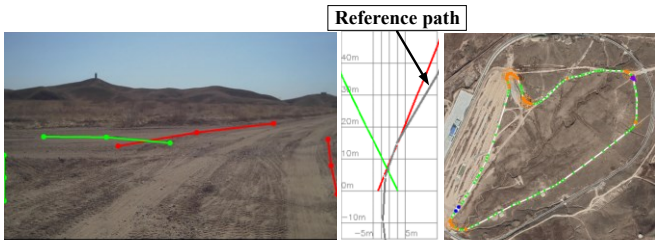

(a) (b) (c)

Fig. 6: (a) Multi-roads detection result. (b) Road selection. (c) The given GNTM.

First according to the current navigation information of the vehicle, the current driving road segment can be extracted from GNTM as a reference path as shown in Fig. 6(b). Then for these road detection results, the road's orientation information is matched with the topological orientation of the current driving road segment from GNTM. And the road with the minimum deviation is selected according to (8).

$$R_{best} = \arg\min_{Ri} \left| \theta_G^i - \theta_{\text{ref}} \right| \tag{8}$$

Where R_i represents the I-th road, θ_G^i is its absolute heading and θ_{ref} is the orientation of the reference guidance route.

C. Path Optimization

There is usually a deviation between the detected road boundaries and the actual road boundaries on the visual image for some image frames in unstructured terrain with blurred

road. As shown in Fig. 7, the dotted line shows the ideal road boundary detection result, and the actual detection result (solid line representation) deviates from the ideal road detection result. More seriously, after perspective transformation, this deviation will be amplified, resulting in a certain degree of oscillations in the road boundary detection result of some certain frames. In the actual autonomous driving of the vehicle, it will cause the instability of vehicle control.

In view of the above problems, on the one hand, fusion processing including previous frames and the current frame can be adopted. By merging historical frames with the current frame in a period of time, it can improve the accuracy and stability of detection results for real-time control. On the other hand, the lateral control of the vehicle need to be constrained within a certain range to avoid the left and right swing of autonomous driving.

(a) (b)

Fig. 7: (a) The T-th frame detection result. (b) The (T+i)-th frame detection result.

Data fusion based on multi-frame detection results over a period of frame can effectively reduce the detection error and control instability caused by single frame detection deviation.

In the specific processing, current road boundaries detection result of each frame is projected on the absolute global frame by using the coordinate transformation shown in (9).

$$\begin{bmatrix} x_G \\ y_G \end{bmatrix} = \begin{bmatrix} x_V \\ y_V \end{bmatrix} + \begin{bmatrix} \sin\theta_V & \cos\theta_V \\ -\cos\theta_V & \sin\theta_V \end{bmatrix} \cdot \begin{bmatrix} x_L \\ y_L \end{bmatrix} \tag{9}$$

Where (x_V, y_V) is the current absolute coordinate position of the vehicle, θ_V is the current heading of driving, (x_L, y_L) is the local coordinate of road boundary point in the vehicle's frame. (x_G, y_G) is the absolute coordinate projected to the global frame.

Then in the next period, according to the inverse transformation of (9), historical frames within a period (T=n) are projected to the current vehicle's frame. The accumulated road boundary points are used to generate the linear equation of current road. This method can effectively improve the robustness of visual road detection result. We adjust the belief ratio of different frames by the parameter λ. In order to make the detection result of the current frame have more influence on the fusion result, λ_0 is usually greater than the others. The set of boundary points are represented as (10):

$$P = \{\lambda_0 \otimes P_{cur}, \lambda_1 \otimes P_{h1}, \lambda_2 \otimes P_{h2}, ..., \lambda_n \otimes P_{hn}\} \tag{10}$$

Where $\lambda_i \otimes P_i = \left(P_i^1, P_i^2, ..., P_i^\lambda\right)^T$ and $P_i = \begin{bmatrix} x_1^i & y_1^i \\ x_2^i & y_2^i \\ x_3^i & y_3^i \end{bmatrix}$.

Then by (5), the road middle-line equation based on fusion optimization can be obtained. According to the road middle-line equation, a reference path can be generated as shown in Fig. 8(b).

Under usual circumstances, direct use of the middle line of boundary for autonomous navigation is likely to cause the lateral control of the vehicle to oscillate, especially when the direction of the detected result is significantly largely deviated from the vehicle's heading. To reduce the jitter of the lateral control, model predictive control is used for path optimization of the generated middle-line. As shown in Fig. 8(c), by optimizing tracking path of the middle-line, the amount of lateral control is constrained to avoid large oscillations.

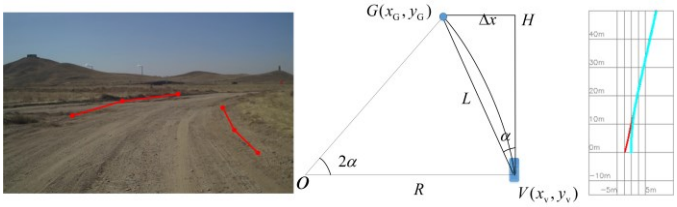

(a) (b) (c)

Fig. 8 Path optimization. (a) Road boundary detection result. (b) Pure tracking model. (c) Path optimization result based on the pure tracking model.

In this paper, the simple two-degree of freedom vehicle model is used as the prediction model for the road middle-line path tracking, and pure tracking algorithm [14] is applied for path tracking control as shown in Fig. 8(b). The vehicle's position denotes as $V(x_v, y_v)$, and the vehicle's heading denotes as $\overrightarrow{VH}$. $G(x_G, y_G)$ is the preview position point, L denotes the actual preview distance, O is the steering center, R is the turning radius and Δx denotes the lateral offset between the vehicle's position and the preview position. The path optimization result is shown in Fig. 8(c). The optimized path is smoother and conforms to the motion of the vehicle.

D. Obstacle Avoidance Analysis

In general, the detected road area is of obstacle-free, it can guarantee driving safely in most scenarios by driving along the middle-line of the detected road. The proposed method can also be combined with LIDAR sensing results to further improve the security of autonomous navigation. Multi-paths generation and cluster analysis algorithm proposed in paper [15] is applied here to implement obstacle avoidance and path optimization. First, a certain number of equidistant lateral offset is generated by panning the reference path. Thus we get multiple candidate reference paths as shown in Fig. 9(c). Then using the pure tracking algorithm combined with LIDAR perception, each candidate path is performed tracking prediction. Finally cluster analysis is performed based on the longitudinal reachable distance of each candidate trajectory. Trajectory with the lowest cost of traffic safety both in

horizontal and vertical direction in the grid map is selected as the execution trajectory as shown in Fig. 9(d).

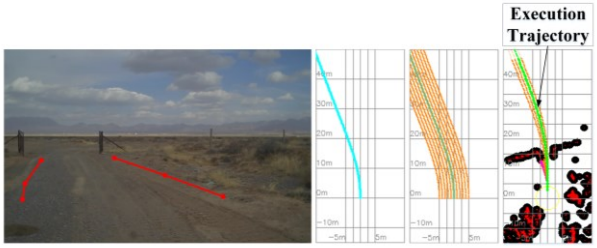

(a) (b) (c) (d)

Fig. 9 Obstacle avoidance analysis. (a) Road boundary detection result. (b) Path optimization of the road midline. (c) Multi-trajectories generation. (d) Selection of execution Trajectories and trajectories tracking.

VI. Experiments

The proposed visual road boundary detection based local path planning algorithm has been tested in a lot of experiments on a self-driving vehicle. The experiment environment includes various terrain environment and different road types in unstructured scenarios. Typical test scenarios are shown in Fig. 10 including straight road, curve road, fork road, as well as road with obstacles such as trees.

The computing platform includes Jetson TX2 and the Advantech embedded computer with Core i7 6600U. The former is used for the deep learning based road boundary recognition. And the latter is used for the processing of different sensor data fusion and path planning. The total time cost is about 120ms per frame from visual data acquisition to the execution of the control command. The maximum speed that can be maintained is up to 18km/h in unstructured scenarios. Fig. 11 shows a complete autonomous navigation task of 8km based on the proposed method. Almost all the road sections are driven based on visual road boundary detection based local path planning without manual intervention. Only a few road segment with sharp turns or in the wide intersection cannot be detected as shown in Fig.11. In this case, autonomous navigation is just based on the given GNTM and the current positioning. And the GNTM play an important role in the selection of the fork road.

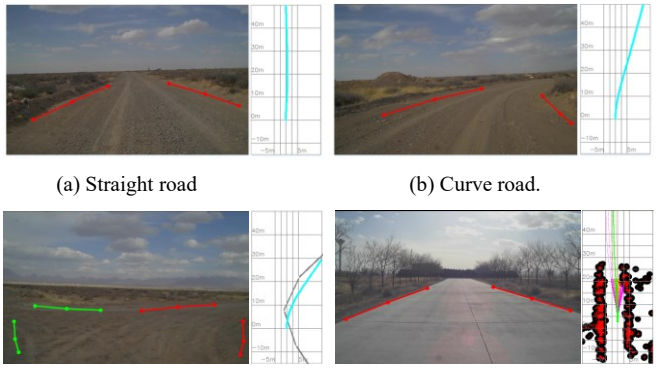

(a) Straight road (b) Curve road.

(c) Fork road. (d) Local path planning with obstacle avoidance.

Fig. 10. Typical test road result.

Although the positive detection rate is up to 97% in our experiments, false detection and missed detection cannot be avoided. For false detection, when the detected road heading has a large deviation with the reference heading based on the GNTM, local path planning based on the GNTM is applied. Meanwhile obstacle detection on both sides of the road by LIDAR can also be used for keeping driving on the road. For missed detection on the straight road, the last valid detection result can be kept for a while by using Kalman filter.

The red dotted line in Fig.11 shows the self-driving trajectories by the proposed method, the trajectories is smooth. Obstacles like trees are random distribution on the road. The self-driving vehicle passed though all these areas safely. The experimental results show that visual road boundary detection based local path planning algorithm has good environmental adaptability and versatility for unstructured terrain. It can reduce the dependence on satellite positioning and is suitable for autonomous navigation in unstructured environments with visual features. Meanwhile by combining the given GNTM and LIDAR perception result, the problem of multi-roads selection and obstacle avoidance can be effectively solved.

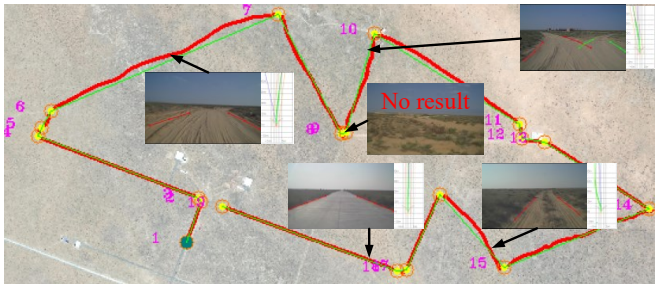

Fig. 11 An autonomous navigation test of 8km based on the proposed method.

VII. Conclusion

In this paper, we have presented a local path planning based on visual road boundary detection. The proposed method can effectively restrain autonomous driving in the middle of the road by detecting the road boundary. It can guarantee the driving stability. In some case, the proposed method can replace autonomous navigation heavily depending on satellite positioning. It is a good solution of local navigation for unstructured road without structured features except visual texture. At the same time, the low cost of visual sensor equipment is of great significance for the development of low-cost unmanned technology.

In our current research work, obstacle avoidance still depends on LIDAR sensor to ensure the safety of autonomous navigation. However, point clouds are discretely distributed in 3-D space, so there are false detections for grasses and general obstacles especially in unstructured environments. In the further research work, we will focus on environmental perception based on visual information. For example, by dealing with color information and texture feature or even by using stereo vision, the accessible area and obstacle area can be distinguished. It is useful to reduce the dependence on LIDAR sensor for its high cost. Meanwhile visual recognition

based environmental perception is useful to improve the scenarios understanding compared with LIDAR sensors. We hope our research work is meaningful for the development of autonomous navigation in the field of robotics.

ACKNOWLEDGMENT

This work was supported in part by National Natural Science Foundation of China (Grand No. 91748211).

REFERENCES

[1] Schwarting W , Alonso-Mora J , Rus D . Planning and Decision-Making for Autonomous Vehicles[J]. Annual Review of Control, Robotics, and Autonomous Systems, 2018, 1(1):annurev-control-060117-105157.

[2] Best A , Narang S , Barber D , et al. [IEEE 2017 IEEE/RSJ International Conference on Intelligent Robots and Systems (IROS) - Vancouver, BC (2017.9.24-2017.9.28)] 2017 IEEE/RSJ International Conference on Intelligent Robots and Systems (IROS) - AutonoVi: Autonomous vehicle planning with dynamic maneuvers and traffic constraints[J]. 2017:2629-2636.

[3] Maturana D, Chou P W, Uenoyama M, et al. Real-Time Semantic Mapping for Autonomous Off-Road Navigation[M]// Field and Service Robotics. 2018.

[4] Bojarski M , Del Testa D , Dworakowski D , et al. End to End Learning for Self-Driving Cars[J]. 2016.

[5] Berger C, Rumpe B. Autonomous driving-5 years after the urban challenge: The anticipatory vehicle as a cyber-physical system[J]. arXiv preprint arXiv:1409.0413, 2014.

[6] Chen C, Seff A, Kornhauser A, et al. Deepdriving: Learning affordance for direct perception in autonomous driving[C]//Proceedings of the IEEE International Conference on Computer Vision. 2015: 2722-2730.

[7] Wang X , Wang J , Zhang Y , et al. 3D LIDAR-Based Intersection Recognition and Road Boundary Detection Method for Unmanned Ground Vehicle[J]. 2015 IEEE 18th International Conference on Intelligent Transportation Systems (ITSC), 2015, IEEE18thInternationalConferenceonIntelligentTransportationSystems(ITSC).

[8] Jiang H , Xiao Y , Zhang Y , et al. Curve path detection of unstructured roads for the outdoor robot navigation[J]. Mathematical and Computer Modelling, 2013, 58(3-4):536-544.

[9] Cai H, Liu E, Liu H, et al. Real-Time Road-Direction Point Detection in Complex Environment[J]. IEICE TRANSACTIONS on Information and Systems, 2018, 101(2): 396-404.

[10] J. Redmon, S. Divvala, R. Girshick, and A. Farhadi, “You only lookonce: Unified, real-time object detection,” arXiv:1506.02640, 2015.

[11] Redmon J, Farhadi A. YOLO9000: Better, Faster, Stronger[C]// IEEE Conference on Computer Vision & Pattern Recognition. 2017.

[12] Redmon J, Farhadi A. YOLOv3: An Incremental Improvement[J]. 2018.

[13] Mezirow J. Perspective Transformation[J]. Adult Education Quarterly, 2014, 28(28):100-110.

[14] Coulter R C. Implementation of the pure pursuit path tracking algorithm[R]. CARNEGIE-MELLON UNIV PITTSBURGH PA ROBOTICS INST, 1992.

[15] Ning Li, Xijun Zhao, Ruina Dang, Bo Su. DF-FS based path planning algorithm with sparse waypoints in unstructured terrain[C]. //IEEE International Conference on Robotics and Biomimetics.2018:1783-1788